HHS Public Access

Author manuscript

Nat Immunol. Author manuscript; available in PMC 2015 March 01.

Published in final edited form as:

Nat Immunol. 2014 September ; 15(9): 884–893. doi:10.1038/ni.2943.

c-Myc-induced transcription factor AP4 is required for CD8+ T cell-mediated host protection

Chun Chou[1], **Amelia K. Pinto**[2], **Jonathan D. Curtis**[1], **Stephen P. Persaud**[1], **Marina Cella**[1], **Chih-Chung Lin**[1], **Brian T. Edelson**[1], **Paul M. Allen**[1], **Marco Colonna**[1], **Erika L. Pearce**[1], **Michael S. Diamond**[1,2,3], and **Takeshi Egawa**[1,*]

[1]Department of Pathology and Immunology, Washington University School of Medicine, Saint Louis, MO 63110

[2]Department of Medicine, Washington University School of Medicine, Saint Louis, MO 63110

[3]Department of Molecular Microbiology, Washington University School of Medicine, Saint Louis, MO 63110

Abstract

Although c-Myc is essential to establish a metabolically active and proliferative state in T cells after priming, its expression is transient. It remains unknown how T cell activation is maintained after c-Myc down-regulation. Here, we identify AP4 as the transcription factor that is induced by c-Myc and sustains activation of antigen-specific CD8$^+$ T cells. Despite normal priming, AP4-deficient CD8$^+$ T cells fail to continue transcription of a broad range of c-Myc-dependent targets. Mice lacking AP4 specifically in CD8$^+$ T cells showed enhanced susceptibility to West Nile virus infection. Genome-wide analysis suggests that many activation-induced metabolic genes are shared targets of c-Myc and AP4. Thus, AP4 maintains c-Myc-initiated cellular activation programs in CD8$^+$ T cells to control microbial infections.

Protective immunity by CD8$^+$ T cells is critical for host defense against many pathogens that cause death or chronic infection. During an acute infection by a virus or intracellular bacterium, antigen (Ag)-specific CD8$^+$ T cells are primed by signals through the T cell receptor (TCR), co-stimulatory molecules and cytokine receptors and undergo rapid expansion, effector differentiation, and memory cell formation[1, 2]. In the priming phase, activated CD8$^+$ T cells grow in size by increasing global gene transcription and protein translation and utilize aerobic glycolysis pathways to produce the energy and materials for biosynthesis prior to cell cycle entry[3, 4, 5, 6, 7]. Previous studies established that the transcription factor (TF) c-Myc is essential for the initiation of the global cellular activation

*Correspondence to: Takeshi Egawa (tegawa@wustl.edu).

ACCESSION CODE: Gene expression omnibus: GSE58081

AUTHOR CONTRIBUTIONS

T.E. designed the study with help with M. Cella, M. Colonna, P.M.A., E.L.P and M.S.D. C.C., A.K.P., J.D.C., S.P.P., C.-c.L., B.T.E. and T.E. performed experiments. C.C., E.L.P., M.S.D. and T.E. analyzed data. T.E. wrote the manuscript with the other authors providing editorial comments.

processes in activated lymphocytes as well as cancer and embryonic stem cells[8, 9, 10, 11]. c-Myc is induced by signals through the TCR and IL-2 receptor (IL-2R)[12] and is essential for the metabolic reprograming and cell growth of T cells[13].

During acute infection, $CD8^+$ T cell expansion persists even after levels of Ag and inflammation wane[4]. While this persistent proliferation may be driven by residual Ag on Ag-presenting cells, other evidence suggests that optimally primed $CD8^+$ T cells continue proliferation after Ag and cytokines decrease to sub-optimal concentrations[14, 15, 16, 17]. Expression of c-Myc is rapidly induced in activated T cells[9, 13]. Its expression, however, does not persist throughout the duration of T cell expansion[9, 18]. These findings suggest that other TFs maintain c-Myc-initiated cellular activation to maximize clonal expansion and effector differentiation of T cells during acute responses to pathogen infection.

We hypothesized that TCR and cytokine receptor signals during the early stage of pathogen infection induce TFs, which program $CD8^+$ T cells for a durable response. Among the cytokines established as important for $CD8^+$ T cell responses, IL-2 sustains clonal expansion *in vitro* and possibly *in vivo*[19, 20, 21], and promotes effector differentiation[20, 22, 23]. In this study, we identified AP4 as a TF regulated by IL-2R signals and demonstrated that AP4 cell-autonomously sustains proliferation of Ag-specific $CD8^+$ T cells in acute infection models. $CD8^+$ T cells lacking AP4 failed to sustain clonal expansion compared to control wild-type (WT) cells, leading to a substantially reduced clonal frequency at the peak of response. Mice lacking AP4 specifically in $CD8^+$ T cells failed to control infection of West Nile virus (WNV) in the central nervous system (CNS), which requires sustained Ag-specific $CD8^+$ T cell responses for host-mediated clearance and survival. Finally, our data suggest that AP4 sustains cellular activity through regulation of a substantial proportion of c-Myc target genes. Thus, our data establish that AP4 regulates the magnitude of acute $CD8^+$ T cell responses to control microbial infection.

RESULTS

AP4 is regulated by TCR and IL-2R signals

Using microarray analysis (GSE58081), we identified ~70 TFs whose expression changed by greater than 1.8-fold in $CD8^+$ T cells following neutralization of IL-2 (Fig. 1a). In addition to known IL-2-regulated genes, *Bcl6* and *Eomes*[23], we identified *Tfap4*, encoding AP4, as an IL-2R signal-dependent gene. AP4 is a basic helix-loop-helix protein that regulates viral gene transcription and *Cd4* gene repression[24, 25, 26]. Although *Tfap4* mRNA expression was reduced modestly upon withdrawal of IL-2, AP4 protein expression was substantially diminished (Fig. 1b,c), suggesting that sustained AP4 expression requires IL-2R signals at both transcriptional and post-transcriptional levels. AP4 expression from retrovirus (RV) also required IL-2R stimulation (Fig. 1d), suggesting its expression regulated predominantly at the post-transcriptional level. The half-life of AP4 protein was two to three hours under permissive (+IL-2) or non-permissive (IL-2 neutralization) conditions (Fig. 1e), with its degradation mediated by the ubiquitin-proteasome pathway (Fig. 1f). AP4 expression was sustained by TCR stimuli or other gamma chain cytokines (IL-7 and IL-15) but not by IL-12 or type I interferons (Fig. 1g). These results suggest that a common pathway converging from TCR and IL-2Rγ chain signaling sustains AP4 protein

expression. Consistently, MEK and p38 MAPK inhibitors U0126 and SB203580, respectively, attenuated the accumulation of AP4 protein in the presence of TCR or IL-2R stimulation (Fig. 1h). To validate the roles of TCR and IL-2R in maintaining AP4 expression *in vivo*, we examined AP4 levels in Ag-specific $CD8^+$ T cells during acute infection with the Armstrong strain of lymphocytic choriomeningitis virus (LCMV-Arm) (Fig. 1i). AP4 protein was expressed highly in Ag-specific $CD8^+$ T cells on days 4 and 5 after infection. The level declined on days 6 and 7 as T cell expansion markedly slowed. In activated $CD8^+$ T cells on day 4.5 after LCMV-Arm infection, AP4 protein was detected specifically in $CD25^{Hi}$ cells, but not in $CD25^{Lo}$ cells, despite similar mRNA levels in both subpopulations (Fig. 1j). Furthermore, Ag-specific $CD8^+$ T cells lacking *Il2ra* expressed reduced amounts of AP4 protein four days after LCMV-Arm infection (Fig. 1k). We conclude that AP4 is regulated post-transcriptionally in $CD8^+$ T cells via signaling through TCR and IL-2R *in vitro* and *in vivo*.

AP4 is required for $CD8^+$ T cell expansion

To assess AP4 functions in immune responses, we infected *Tfap4*$^{-/-}$ and congenic wild-type (WT) C57BL/6 mice with LCMV-Arm and examined expansion and differentiation of $CD8^+$ T cells. At the peak of response, numbers of total $CD8^+$ T cells and $KLRG1^+$ terminally differentiated $CD8^+$ T cells[1] were reduced by ~70% and 90%, respectively, in *Tfap4*$^{-/-}$ compared to WT mice (Fig. 2a,c). T cells specific for the gp(33–41) epitope also were decreased by 80% and, among them, $KLRG1^+$ effector cells were diminished by 90% in *Tfap4*$^{-/-}$ compared to WT mice (Fig. 2b,d). To determine whether the requirement for AP4 was $CD8^+$ T cell-intrinsic, we deleted a loxP-flanked *Tfap4* allele specifically in $CD8^+$ T cells using a CD8-Cre transgenic deleter[27] (Supplementary Fig. 1a,b). We observed a similar reduction in numbers of total, $KLRG1^+$ and gp(33–41)-specific $CD8^+$ T cells in *Tfap4*$^{-/-}$ and *Tfap4*$^{F/F}$ CD8-Cre^+ mice (Supplementary Fig. 1c,d), indicating that the AP4 requirement is $CD8^+$ T cell-intrinsic. $CD8^+$ T cell clonal expansion and effector differentiation also were reduced in *Tfap4*$^{-/-}$ mice infected with *Listeria monocytogenes* expressing ovalbumin (Lm-Ova) (Supplementary Fig. 2a,b). Memory cells were generated and maintained comparably between *Tfap4*$^{-/-}$, *Tfap4*$^{F/F}$ CD8-Cre^+ and WT mice following infection with LCMV-Arm or Lm-Ova (Supplementary Fig. 3a-d). However, expansion of *Tfap4*$^{-/-}$ memory T cells was diminished upon secondary challenge (Supplementary Fig. 3e-h). Thus, AP4 is essential for expansion of Ag-specific $CD8^+$ T cells both in primary and recall responses.

AP4 sustains $CD8^+$ T cell clonal expansion

To compare expansion of *Tfap4*$^{-/-}$ and WT $CD8^+$ T cells in an identical environment, we generated *Tfap4*$^{-/-}$ mice expressing a $V_\alpha2^+V_\beta8^+$ TCR transgene specific for gp(33–41) (P14) (ref. [28]). A 1:1 mixture of $V_\alpha2^+V_\beta8^+$ naive $CD8^+$ T cells from *Tfap4*$^{-/-}$ (Thy-1.2/CD45.2) and WT (Thy-1.1/CD45.2) P14 mice was adoptively transferred to congenic host CD45.1 mice. Prior to infection with LCMV-Arm, the ratio of *Tfap4*$^{-/-}$ to WT P14 T cells remained approximately 1:1 in the spleen (Fig. 3a). This result is consistent with comparable frequencies of $CD8^+$ T cells in various tissues in *Tfap4*$^{-/-}$ and WT mice under steady state conditions (Fig. 3b). To determine whether AP4 was required for initial proliferation of P14 T cells, we labeled donor P14 T cells with carboxyfluorescein succinimidyl ester (CFSE)

followed by adoptive transfer and infection of host mice with LCMV-Arm. On day 3 after infection, both *Tfap4*$^{-/-}$ and WT P14 T cells diluted CFSE to undetectable levels (Fig. 3c), which was consistent with the comparable numbers of P14 T cells in the spleen and the frequencies of bromodeoxyuridine (BrdU)$^{+}$ cells following a pulse labeling (Fig. 3d-g). These results establish that AP4 is dispensable for initial proliferation of CD8^{+} T cells during the Ag-specific response. Despite the rapid early expansion, the absolute number of *Tfap4*$^{-/-}$ donor cells was substantially reduced compared to WT donor cells at the peak of the response (Fig. 3d-f). Although *Tfap4*$^{-/-}$ cells continued to proliferate until day 7 post-infection, they failed to maintain rapid proliferation rates, as judged by BrdU pulse labeling on day 4 and later (Fig. 3g). Because CD8^{+} T cells divide 6-7 times per day during a response to acute infection[29], the effect of mild but continued reduction in BrdU incorporation rates could result in a greater than 90% reduction in clonal expansion of *Tfap4*$^{-/-}$ donors compared to WT cells over 4 days (Fig. 3e,g). We also observed reduced clonal expansion, BrdU incorporation, and mTOR pathway activation in *Tfap4*$^{-/-}$ OT-I T cells following Lm-Ova infection (Supplementary Fig. 2c-e). We did not, however, observe changes in the frequency of AnnexinV-binding cells between *Tfap4*$^{-/-}$ and WT P14 T cells on day 6 (Fig. 3h,i), or ratios between *Tfap4*$^{-/-}$ and WT P14 T cells in various compartments on day 7 after LCMV-Arm infection (Fig. 3j). These results suggest no substantial difference in apoptosis or trafficking of Ag-specific T cells *in vivo*. Furthermore, it is unlikely that AP4 regulates TCR sensitivity *per se*, since *Tfap4*$^{-/-}$ and WT OT-I T cells proliferated at similar rates, and comparably produced IFN-γ in response to Ag *in vitro* (Supplementary Fig. 2f-h). However, *Tfap4*$^{-/-}$ cells were outcompeted in numbers by co-cultured WT cells and failed to blast when kept for a longer duration with low concentration of peptide. These results suggest that AP4 is required for sustained T cell proliferation after TCR stimulation.

Protection against WNV infection requires AP4

We next tested the contribution of AP4 to CD8^{+} T cell-mediated protection against a lethal infection by utilizing the WNV infection model. WNV is a virulent zoonotic virus causing fatal encephalitis in humans and mice[30, 31]. CD8^{+} T cells are required for clearance of WNV in both the spleen and CNS[32]. To determine whether AP4 was required for protection against WNV infection in a CD8^{+} T cell-dependent manner, we infected *Tfap4*$^{F/F}$ CD8-Cre^{+} mice and age-matched control *Tfap4*$^{F/F}$ Cre^{-} mice with WNV. While the majority of *Tfap4*$^{F/F}$ Cre^{-} mice survived, all *Tfap4*$^{F/F}$ CD8-Cre^{+} mice died between days 8 and 13 (Fig. 4a), which was similar to the lethality observed in mice lacking CD8^{+} T cells[32]. *Tfap4*$^{F/F}$ CD8-Cre^{+} mice sustained higher viral loads in the brain compared to control mice on day 9 post-infection (Fig. 4b), indicating that AP4 expression in CD8^{+} T cells is essential for the control of WNV in the CNS. Ag-specific CD8^{+} T cell expansion was diminished in WNV-infected *Tfap4*$^{-/-}$ and *Tfap4*$^{F/F}$ CD8-cre^{+} mice compared to control WT mice in the spleen on day 7 after infection (Supplementary Fig. 4). However, AP4 was dispensable for control of WNV in the spleen (Fig. 4c). Consistent with this observation, no differences in LCMV-Arm or Lm-Ova burden were detected in peripheral tissues following infection presumably because clearance of these pathogens begins at an early phase of the acute response (Fig. 2e and Supplementary Fig. 2i). In contrast, AP4 is required for host protection against WNV

infection in the CNS, and AP4-mediated sustained activation of Ag-specific $CD8^+$ T cells may be critical for control of certain CNS pathogens.

AP4 sustains T cell activation

Upon T cell priming, c-Myc activates aerobic glycolysis and amplifies global gene transcription and protein synthesis, leading to cell size growth and metabolic reprogramming[6, 9, 13, 33]. c-Myc expression was induced rapidly after TCR stimulation, followed by AP4 up-regulation in $CD8^+$ T cells (Supplementary Fig. 5a,b). c-Myc was essential for AP4 up-regulation in activated $CD8^+$ T cells at both protein and mRNA levels (Fig. 5a). In agreement with a prior study[34], c-Myc bound to the *Tfap4* locus in activated $CD8^+$ T cells (Supplementary Figs. 5c and 6e), further suggesting that AP4 expression is augmented by c-Myc through direct binding. In contrast to defective cell growth and metabolic changes in *Myc*-deficient T cells[13], activated *Tfap4*$^{-/-}$ $CD8^+$ T cells underwent normal blast development accompanied by active glycolysis *in vitro* (Supplementary Fig. 5d-f). Moreover, *Tfap4*$^{-/-}$ and WT Ag-specific T cells were of comparable size three days after LCMV-Arm or Lm-Ova infection (Fig. 5b, and Supplementary Fig. 5g). Differences in gene expression between *Tfap4*$^{-/-}$ and WT $CD8^+$ T cells either three days after activation *in vitro* or two days after Lm-Ova infection were substantially smaller than that observed at later time points with few genes relevant to T cell activation altered (Supplementary Fig. 5h). Thus, AP4 is dispensable for establishment of the c-Myc-dependent cellular response to T cell activation. However, at later time points (days 4 and 6), *Tfap4*$^{-/-}$ Ag-specific $CD8^+$ T cells were smaller in size than control cells (Fig. 5b,c and Supplementary Fig. 5g). The size difference between *Tfap4*$^{-/-}$ and control cells coincided with c-Myc down-regulation in Ag-specific $CD8^+$ T cells after Lm-Ova infection (Fig. 5d,e). A small fraction of OT-I T cells primed by Lm-Ova infection up-regulated c-Myc protein as determined using the c-Myc–GFP fusion protein knock-in allele[35]. Activated OT-I T cells uniformly expressed c-Myc–GFP as they expanded in size until day 3 (Fig. 5d). Although they continued to proliferate and only slowly reduced cell size on day 4, c-Myc–GFP was down-regulated by 95% compared to day 2 and by 90% compared to day 3 (Fig. 5d,e). In comparison, AP4 expression in WT cells also was up-regulated following c-Myc induction and began to decline on day 3 (Fig. 5d). In contrast to the rapid c-Myc decay, AP4 protein was still detected on day 4 (**3**), suggesting that AP4 expression persists longer than c-Myc. Total RNA content per cell also was reduced in *Tfap4*$^{-/-}$ compared to WT OT-I T cells on day 4 (Fig. 5f). Furthermore, basal aerobic glycolysis and the maximum glycolytic capacity, as measured by extracellular acidification rates (ECAR)[36], were significantly reduced in *Tfap4*$^{-/-}$ compared to WT OT-I cells recovered from the same host mice on days 4 and 6 after Lm-Ova infection (Fig. 5g). Consistently, expression of key glycolytic enzymes normalized to a per cell basis by using spiked-in control RNA[37] was reduced by 30 to 60% and by 75 to 80% in *Tfap4*$^{-/-}$ compared to WT OT-I T cells on days 4 and 6 post-infection, respectively (Fig. 5h). These results indicate that AP4 is required for sustained expression of glycolytic genes and suggest that AP4 sustains T cell activation after c-Myc down-regulation.

AP4 sustains c-Myc-initiated global cellular activity

To further define the AP4 requirement in maintenance of the c-Myc-initiated T cell activation, we analyzed gene expression in *Tfap4*$^{-/-}$ and WT OT-I T cells activated *in vivo* using microarray (GSE58081) at the time point in which we detected cell size differences. For accurate assessment of gene expression, we spiked the cellular RNA with a mixture of control RNAs according to the cell number and then profiled cell number-normalized gene expression in *Tfap4*$^{-/-}$ and WT OT-I T cells[9, 10]. Consistent with the smaller size and reduced RNA content of *Tfap4*$^{-/-}$ cells, global gene expression in *Tfap4*$^{-/-}$ cells, as determined by the slopes of scatter plots, was reduced compared to WT cells (Fig. 6a-b). We identified 1,784 genes that showed greater than 1.8-fold difference between *Tfap4*$^{-/-}$ and WT OT-I cells four days after Lm-Ova infection. A pathway analysis highlighted an enrichment of the 1,784 genes in those related to metabolism, transcription and translation (Fig. 6c). To determine whether these genes were directly regulated by AP4, c-Myc or both, we performed chromatin immunoprecipitation (ChIP) analysis using anti-AP4 and anti-c-Myc antibodies and profiled AP4- and c-Myc-bound genes in activated CD8^{+} T cells (Supplementary Fig. 6, GSE58081). Unbiased analysis of 7,000 statistically significant peaks of AP4 or c-Myc binding remarkably revealed that more than 50% of AP4 and c-Myc peaks overlapped at the gene level (Fig. 6d). Furthermore, nearly a quarter (479 genes) of the 1,784 genes differentially expressed between *Tfap4*$^{-/-}$ and WT OT-I T cells were bound by both AP4 and c-Myc (Fig. 6d). These AP4-c-Myc shared target genes were highly enriched in those annotated in metabolism, transcription and translation pathways (Fig. 6c and Supplementary Fig. 6e). The majority of these 479 genes were up-regulated on day 2 after Lm-Ova infection in WT OT-I cells expressing both c-Myc and AP4, remained highly expressed on day 4 when c-Myc levels waned, and were eventually down-regulated on day 6 following the decline of AP4, suggesting that AP4 regulated these genes as c-Myc expression decayed (Fig. 6e). Because expression of these 479 genes was not different between *Tfap4*$^{-/-}$ and WT OT-I T cells on day 2 post-infection (Supplementary Fig. 5h), the altered expression of these genes on day 4 may explain the phenotypes observed in *Tfap4*$^{-/-}$ OT-I T cells. Since the ChIP analysis was performed using cells co-expressing AP4 and c-Myc, we further tested whether AP4 still bound to these loci after c-Myc down-regulation using CD25^{+} P14 T cells five days after LCMV-Arm infection. Although c-Myc was down-regulated in P14 T cells on day 5 compared to earlier time points (Fig. 6f), the majority of previously identified AP4-c-Myc-bound loci retained AP4 binding (Fig. 6g). These results suggest that c-Myc-induced AP4 expression is required for sustained transcription of c-Myc target genes through direct binding.

AP4 supplements c-Myc function

Our data thus far suggest that AP4 and c-Myc have overlapping functions in activated CD8^{+} T cells. To determine whether AP4 was dispensable if c-Myc expression is sustained, we retrovirally expressed a stabilized form of c-Myc (T58A mutant[38, 39]) in *Tfap4*$^{-/-}$ OT-I T cells in a culture system that recapitulates the cell size difference between *Tfap4*$^{-/-}$ and WT cells. In this assay, *Tfap4*$^{-/-}$ and WT OT-I T cells were primed with anti-CD3 and anti-CD28 antibodies for two days and transferred to a culture of irradiated splenocytes pulsed with 1 pM of Ova peptide for 24 hours. Ectopic expression of c-Myc(T58A) or AP4 itself in

Tfap4$^{-/-}$ OT-I T cells rescued the cell size defects under these conditions (Fig. 7a,b). Overexpression of c-Myc(T58A) or AP4 also restored glycolysis, BrdU incorporation, and expression of a subset of AP4-c-Myc-regulated genes (Fig. 7c-e). To determine whether c-Myc(T58A) expression restored clonal expansion of *Tfap4*$^{-/-}$ CD8^{+} T cells *in vivo*, we adoptively transferred c-Myc(T58A)- or AP4-transduced naive *Tfap4*$^{-/-}$ OT-I T cells and empty-RV-transduced WT OT-I T cells into congenic hosts followed by Lm-Ova infection. Although retroviral expression of AP4 in *Tfap4*$^{-/-}$ OT-I T cells fully restored clonal expansion and KLRG1 expression, c-Myc(T58A) expression only partially restored clonal expansion (Fig. 7f-h). Nevertheless, c-Myc(T58A) expression increased size and BrdU incorporation of *Tfap4*$^{-/-}$ OT-I cells comparably to AP4 ectopic expression (Fig. 7i,j). These results suggest that AP4 and c-Myc have partially overlapping functions in regulating T cell activation and that a temporal switch from c-Myc to AP4 is necessary for optimal CD8^{+} T cell expansion.

To determine whether AP4 ectopic expression correspondingly rescued the defects of *Myc*-deficient cells, we retrovirally expressed AP4 in CD8^{+} T cells in which c-Myc was inducibly deleted[40, 41]. To express AP4, we infected CD8^{+} T cells from *Myc*$^{F/F}$ *ROSA26*-CreER^{T2} (*Myc*$^{-/-}$) and control *Myc*$^{F/+}$ Cre^{-} or *Myc*$^{+/+}$ *ROSA26*-CreER^{T2} mice with RV following twenty-four-hour stimulation *in vitro*, followed by a treatment with 4-hydroxytamoxifen (4OHT) under resting conditions for two days. Subsequently, proliferation and gene expression of transduced cells were tested upon re-stimulation (Supplementary Fig. 7a-c). Retroviral c-Myc expression rescued, albeit partially, proliferation and size increase of *Myc*$^{-/-}$ cells (Supplementary Fig. 7d), presumably because of a delay in expression of RV-derived c-Myc compared to endogenous c-Myc upon re-stimulation (Supplementary Fig. 7c). In contrast, AP4 ectopic expression failed to rescue the defects of *Myc*$^{-/-}$ cells (Supplementary Fig. 7d). Accordingly, gene expression profiling revealed little difference between AP4- and empty RV-transduced *Myc*$^{-/-}$ cells and partially rescued gene expression by c-Myc transduction (Supplementary Fig. 7e). These results indicate that AP4 requires prior expression of c-Myc to mediate its effects. Thus, AP4 functionally supplements c-Myc activity to prolong activation of CD8^{+} T cells.

DISCUSSION

Our study defines a critical role of AP4 in regulating clonal expansion and antiviral function of CD8^{+} T cells. AP4 regulates the maintenance but not initiation of rapid clonal expansion after priming. AP4 is dispensable for control of LCMV-Arm or Lm-Ova infection as clearance of these microbes occurs rapidly and full clonal expansion of Ag-specific CD8^{+} T cell is not necessary. In contrast, AP4 expression in CD8^{+} T cells is essential for protection against neurotropic WNV infection because control of WNV in the CNS requires sustained activity of Ag-specific CD8^{+} T cells. The increased susceptibility could be due to reduced clonal expansion leading to fewer cells reaching the tissue (quantitative defects) or to defective differentiation as effector cells (qualitative defects). Our data suggest that AP4 is required predominantly for sustained rapid proliferation.

Mechanistically, there are two major possible interpretations of AP4 function in regulating acute CD8^{+} T cell responses. One interpretation is direct regulation of genes essential for T

cell activation by AP4. Identification of AP4- and c-Myc–bound genes in $CD8^+$ T cells revealed substantial overlap between targets of the two TFs. Combined analysis of ChIP and gene expression data showed that approximately a quarter of the differentially expressed genes in *Tfap4*$^{-/-}$ cells were shared binding targets of AP4 and c-Myc. When we specifically examined a subset of the 1,748 genes, which were annotated in metabolism, general transcription or translation pathways, AP4 and c-Myc shared targets were further enriched (~75%), supporting the hypothesis that AP4 contributes to maintenance of T cell activation by regulating these genes. AP4 was dispensable for initial up-regulation of these genes upon T cell priming because these pathways are initially activated by c-Myc. In contrast, after c-Myc down-regulation during the late phase of the acute response, the contribution of AP4 to the regulation of these genes may become critical for the maintenance of expression. AP4 binds to these loci not only in $CD8^+$ T cells activated *in vitro*, but also in those activated *in vivo* after c-Myc expression wanes. With respect to cellular carbohydrate metabolism, the differentially expressed genes were enriched for enzymes but not transporters, suggesting the altered glucose utilization in *Tfap4*$^{-/-}$ $CD8^+$ T cells results from defective glycolysis rather than its uptake. In contrast, since many genes encoding enzymes for glutaminolysis, amino acid transporters, and components of protein translation machinery were down-regulated in *Tfap4*$^{-/-}$ $CD8^+$ T cells, their smaller cell size likely reflects reduced protein synthesis from defects at multiple stages. Since expression of *Hif1a* and components of the mTOR pathway was not reduced, the diminished activity of the mTOR pathway may be regulated indirectly by AP4.

As an alternative explanation, AP4 might indirectly sustain activity of T cells through sensitizing T cell activation independent of c-Myc. Sensitivity to extrinsic stimuli may not be important for initial activation of $CD8^+$ T cells in the presence of abundant Ag or inflammatory cytokines. However, it may be critical in the late phase of the $CD8^+$ T cell response *in vivo* due to declines in Ag and cytokine concentrations. Under these circumstances, *Tfap4*$^{-/-}$ cells might prematurely lose activation, leading to their reduced metabolic activity and clonal expansion. A previous study using *Listeria* expressing altered Ova peptide ligands demonstrated that duration and magnitude of Ag-specific $CD8^+$ T cell responses *in vivo* are determined by affinity between TCR and peptide ligands[42]. Compared to Lm-Ova expressing the canonical SIINFEKL epitope, engineered strains expressing low affinity variant epitopes induced reduced clonal expansion of OT-I T cells at the peak despite normal initial activation. Although these phenotypes are similar to those in *Tfap4*$^{-/-}$ mice, there are differences. Infection by *Listeria* expressing low affinity ligands shortens the duration of clonal expansion by triggering earlier contraction and also generates reduced numbers of memory cells after the clearance of the infection[42]. We observed neither of these phenotypes in *Tfap4*$^{-/-}$ mice after infection with Lm-Ova or LCMV-Arm.

Although we favor the former interpretation of AP4-dependent maintenance of c-Myc-regulated genes, the two models are not mutually exclusive. Regardless, our results indicate that c-Myc-induced AP4 expression is essential for maximal clonal expansion and sustained T cell activity in a temporally regulated manner.

In conclusion, our study demonstrates that AP4 is critical for regulation of $CD8^+$ T cell-mediated acute anti-pathogen responses by sustaining metabolic gene expression in the post-

Myc phase. Activated T cells utilize AP4 to maintain their activated states under conditions of threshold signaling for complete elimination of pathogens.

ONLINE METHODS

Mice

Mice harboring a loxP-flanked *Tfap4* allele were generated in 129P2/Ola-derived E14TG2a ES cells essentially as described (Supplementary Fig. 1a)[24]. *Tfap4*$^{-/-}$ mice were described previously[24]. Both AP4 mutant strains were backcrossed to C57BL6 mice for more than 10 generations before intercrossing or breeding to other transgenic mice. *Myc*-flox mice and c-Myc-GFP fusion protein knock-in mice were described previously[35, 40]. C57BL6 and B6-Ly5.2 (CD45.1) mice were purchased from the National Cancer Institute. OT-I transgenic[43], *Tcra*$^{-/-}$ (ref. [44]), *Il2ra*$^{-/-}$ (ref. [45]), *ROSA26*-CreER^{T2} (ref. [41]) and B6-Thy-1.1 mice were purchased from the Jackson Laboratory and P14 transgenic mice[28] were purchased from Taconic. *Il2ra*$^{-/-}$ P14 T cells were collected from mixed bone marrow chimeric mice reconstituted with a mixture of bone marrow cells from *Il2ra*$^{-/-}$ (Thy-1.2) and WT (Thy-1.1) P14 mice. CD8-Cre mice were generated previously in the C57BL6 background[27]. All mice were maintained in a specific pathogen free facility at Washington University in St. Louis, and all experiments were performed according to the protocol approved by Washington University's Animal Studies Committee. All mice were analyzed at 6 – 14 weeks of age, and both sexes were included without randomization or blinding.

Infection Experiments

LCMV-Arm stocks were prepared by infecting BHK cells and titering culture supernatants by plaque assay on Vero cells. Mice were infected with 2×10^5 plaque forming units (PFU) of LCMV-Arm by intraperitoneal injection. Lm-Ova was inoculated intravenously at a dose of 1×10^4 colony-forming units (CFU). Infection with WNV (New York 1999 strain) was performed as previously described[32]. For adoptive transfer experiments, $CD44^-CD62L^+V_\alpha2^+V_\beta5^+$ OT-I or $CD44^-CD62L^+V_\alpha2^+V_\beta8^+$ P14 donor T cells were purified by fluorescence activated cell sorting, and 5×10^5 (for day 3 analysis), 1 to 2×10^4 (for day 4 analysis), or 1 to 3×10^4 (for days 5 to 12 analysis) cells were transferred intravenously to host mice one day before infection. All experiments using infectious agents were performed in biosafety level 2 and 3 facilities according to the protocols approved by Washington University Institutional Biological and Chemical Safety Committee.

Flow Cytometry

Single cell suspensions were prepared by disrupting spleens manually with frosted glass slides followed by erythrocyte lysis with Ammonium-Chloride-Potassium solution, or by digesting mesenteric lymph nodes, liver, lung and kidney with collagenase B and D (Roche) followed by purification using Percoll gradient (GE Healthcare Life Sciences). For sorting of naive $CD8^+$ T cells, splenocytes were initially depleted of $B220^+$ cells using magnetic beads (Life Technologies) and then stained with monoclonal antibodies prior to sorting $CD62L^+CD44^-CD8^+CD4^-$ cells using a FACS AriaII (BD Biosciences). For analysis, cells were stained with monoclonal antibodies, H-2D^b–gp(33–41) (Beckman Coulter), or H2-K^b–Ova single chain tetramer and analyzed using a FACS LSRII (BD Biosciences) with DAPI

staining to exclude dead cells. Data were analyzed using FlowJo software (Tree Star Inc.). All antibodies were purchased from Biolegend. For intracellular staining for AP4, cells were fixed with 2% paraformaldehyde (PFA) for 10 minutes, permeabilized with ice-cold 100% methanol for 30 minutes, and then stained for markers with fluorochrome-conjugated monoclonal antibodies and for AP4 with affinity-purified anti-AP4 polyclonal antibody[24] at a concentration of 1.25 μg/ml, and Alexa-647 conjugated anti-rabbit IgG secondary antibody (Cell Signaling). For detection of phosphorylated S6 (p-S6) ribosomal protein, cells were fixed with PFA, permeabilized with methanol, and stained for surface markers and p-S6 with an anti-p-S6 antibody (Cell signaling 4858) and Alexa-647 conjugated anti-rabbit IgG secondary antibody (Cell Signaling).

BrdU labeling

At different time points after infection mice were administered with 1 mg BrdU by i.p. injection two hours before euthanasia. BrdU incorporation was analyzed using an APC-BrdU Flow Kit (BD Biosciences) according to the manufacturer's instruction. For proliferation assays *in vitro*, cells were cultured in media containing 10 μM BrdU for 1 hour prior to analysis.

In vitro T cell stimulation

Naive $CD8^+$ T cells were cultured in RPMI supplemented with 10% fetal bovine serum (Life Technologies) in the presence of soluble anti-CD3 (145-2C11, Biolegend) and anti-CD28 (37.51, Bio × Cell) at 0.1 μg/ml and 1 μg/ml, respectively, unless otherwise specified, in multi-well tissue culture plates coated with rabbit anti-hamster IgG (MP Biomedicals). For retroviral transduction of activated T cells, viral supernatants were prepared by transfecting PlatE cells[46] with TransIT 293 (Mirus Bio) and primed T cells were spinoculated following overnight stimulation as described previously[24]. To retrovirally transduce $CD8^+$ T cells without TCR stimulation, naive $CD8^+$ T cells were cultured in the presence of IL-7 (10 ng/ml, Peprotech) and IL-15 (100 ng/ml, Peprotech) for 2 days prior to spinoculation. For IL-2 blockade, 2 μg/ml of anti-IL-2 (JES6-1A12, Biolegend) was added to the culture.

Real-time qRT-PCR

RNA was extracted using Trizol (Life Technologies), and reverse transcribed using qScript supermix (Quanta Bio). Real-time qRT-PCR was performed using DyNAmo ColorFlash SYBR green qPCR mix (Thermofisher) and LightCycler 480 (Roche). Quantities of transcripts were normalized against 18S ribosomal RNA (rRNA) unless specificed otherwise. Primer sequences are available upon request. For quantitation of gene expression normalized against spiked-in RNA, 1 μL of 1:1,000 diluted External RNA Controls Consortium (ERCC) RNA Spike-In Control Mixes (Ambion) was added to total RNA extracted from 1×10^5 cells prior to reverse-transcription. The mixed RNA was used for reverse-transcription and real-time PCR quantitation.

Microarray Analysis

Total RNA was extracted with a Nucleospin RNA XS extraction kit (Macherey-Nagel). 5 to 50 ng of total RNA was amplified using PicoSL RNA amplification kit (Nugen) and biotinylated with Encore biotin module (Nugen). Labeled RNA was hybridized to Mouse Gene 1.0ST microarray (Affymetrix) according to the manufacturer's instruction. For each experiment, RNA was prepared from two to three biological replicates, amplified, labeled and hybridized in a single experiment. Data were analyzed using Arraystar (DNA Star) with Robust Multi-array Average (RMA) normalization[47]. For spiked-in microarray analysis, ERCC RNA Spike-In Control Mixes were added as described above followed by RNA amplification, labeling and hybridization. CEL files were generated using a modified CDF file provided by Affymetrix. Data were initially normalized by RMA and signal intensities were further converted by formula obtained from linear regression of signals for spiked-in control RNA between samples.

Chromatin Immunoprecipitation

$CD8^+$ T cells were purified from C57BL6 mice by positive selection with FlowComp CD8 Dynabeads (Life Technologies). Purified $CD8^+$ T cells were stimulated with anti-CD3 and anti-CD28 antibodies for 2 days, and fixed with 1% PFA for 10 minutes at room temperature. Chromatin shearing and immunoprecipitation were performed as described previously[48]. Anti-AP4 antibody was previously described[24]. Anti-c-Myc antibody (sc-764) and anti-phosphorylated RNA polII antibodies (ab5095 and ab5131) were purchased from Santa Cruz and Abcam, respectively. After immunoprecipitation, DNA was purified with a purification kit (Sigma), and 1-10 ng of DNA was used for library construction followed by 50 bp single read sequencing on HiSeq2000 (Illumina). Sequence tags were mapped onto the NCBI37/mm9 assembly of mouse genome using Bowtie2 (ref.[49]) with the default setting. BedGraph histograms normalized to 1×10^7 reads were generated using the Homer package[50] (http://biowhat.ucsd.edu/homer/ngs/) and visualized in the IGV browser (http://www.broadinstitute.org/igv/). Peak calling was performed using Homer with a -style factor option and Poisson *P*-value cut-off of 1e-65 for AP4 and 5e-9 for c-Myc to extract top 7,000 statistically significant peaks. For analysis of overlapping binding targets and binding motifs, 7,000 AP4 binding peaks filtered by $P < 1.5e\text{-}65$ and 7,000 c-Myc-binding peaks ($P < 5e\text{-}9$) were analyzed.

Metabolic Measurements

Extracellular acidification rates (ECARs) were measured using a Seahorse XF96 Analyzer (Seahorse Bioscience) essentially as described[36]. Briefly, $CD8^+$ T cells were purified from uninfected mice (for naive) or chimeric mice transferred with a mixture of *Tfap4*$^{-/-}$ and control WT OT-I T cells and infected with 1×10^4 CFU of Lm-Ova. To prepare *in vitro* activated $CD8^+$ T cells, purified naive $CD8^+$ T cells were activated with anti-CD3 and anti-CD28 antibodies without exogenous IL-2 for 24 hours. 0.15×10^6 cells/well of $CD8^+$ T cells from three biological replicates were seeded onto a 96 well plate and ECARs were measured in duplicate in XF media (non buffered RPMI 1640 containing 25 mM glucose, 2 mM L-glutamine, and 1 mM sodium pyruvate) under basal conditions and in response to 1 μM

oligomycin. Experiments were repeated three times for *in vivo* activated $CD8^+$ T cell samples and four times for naive and *in vitro* activated $CD8^+$ T cells.

Immunoblotting

Whole cell extracts were prepared by lysing cells in Laemmli buffer containing 1% SDS and 2% 2-mercaptoethanol. Lysates from equal numbers of cells were separated by 8 or 10% SDS PAGE, transferred to PVDF membranes (GE Healthcare), incubated with primary antibodies and detected with HRP-conjugated species-specific anti-immunoglobulin light chain antibodies (Jackson ImmunoResearch) and a Luminata HRP substrate (Millipore). Anti-HDAC1 (Abcam, ab7028) and anti-Tubulin beta (Developmental Studies Hybridoma Bank, University of Iowa) were used as loading controls. Anti-AP4 antibody was previously described[24]. The following antibodies were purchased: anti-c-Myc (Cell Signaling, 9402S), anti-phospho STAT5 (PY694) (BD Biosciences, 611964), anti-Blimp-1 (Genscript, A01647-40), anti-T-bet (Santa Cruz, sc-21003). For translation inhibition and proteasome inhibition, 10 μM of cycloheximide (Sigma) or MG-132 (Sigma) was added to the cell culture. For inhibition of signaling pathways, 20 nM of U0126 (Cayman Chemical), 10 μM of SB203580 (Cayman Chemical), 50 nM of wortmannin (Cayman Chemical), 5 nM of FK506 (Cayman Chemical), or 2.5 nM of rapamycin (Cayman Chemical) was added to the cell culture.

Statistical Analysis

P values were calculated with unpaired two-tailed Student's *t*-test for two group comparisons and with one-way ANOVA for multiple group comparisons with the Tukey post-hoc test in Prism 6 (Graphpad) unless otherwise specified. *P* values < 0.05 were considered significant.

Supplementary Material

Refer to Web version on PubMed Central for supplementary material.

ACKNOWLEDGMENTS

We thank M. J. Bevan (University of Washington, Seattle, WA) for Lm-Ova, I. Taniuchi (RIKEN, Yokohama, Japan) and D. R. Littman (New York University, New York, NY) for CD8-Cre mice, B. P. Sleckman (Washington University School of Medicine, St. Louis) for c-Myc–GFP knock-in mice, F. W. Alt (Harvard Medical School, Boston, MA) and D. R. Green (St. Jude Children's Research Hospital, Memphis, TN) for *Myc*-flox mice, T. Hansen (Washington University School of Medicine, St. Louis, MO) for the H-$2K^b$–Ova single chain tetramer, S. Hsiung, J. Govero and M. J. Sunshine for technical assistance, E. Oltz, C.-s. Hsieh and D. R. Littman for discussions and critical reading of the manuscript. This study was supported by the Lucille P. Markey Pathway Program (C.C.), a Burroughs Wellcome Fund Career Award for Medical Scientists (B.T.E.), the McDonnell International Scholars Academy at Washington University (C.-C.L.) and grants from the National Institutes of Health (NIH) (R01 AI097244 to T.E., and U54 AI081680 to M.S.D.), and the Edward Mallinckrodt Jr. Foundation (T.E.). This study also was supported in part by an NIH grant to the Rheumatic Diseases Core Center (P30 AR048335) and by the Washington University Institute of Clinical and Translational Sciences grant UL1 TR000448 from the National Center for Advancing Translational Sciences (NCATS) of NIH.

References

1. Kaech SM, Wherry EJ. Heterogeneity and cell-fate decisions in effector and memory CD8+ T cell differentiation during viral infection. Immunity. 2007; 27(3):393–405. [PubMed: 17892848]

2. Zhang N, Bevan MJ. CD8(+) T cells: foot soldiers of the immune system. Immunity. 2011; 35(2): 161–168. [PubMed: 21867926]
3. Chang CH, Curtis JD, Maggi LB Jr. Faubert B, Villarino AV, O'Sullivan D, et al. Posttranscriptional control of T cell effector function by aerobic glycolysis. Cell. 2013; 153(6): 1239–1251. [PubMed: 23746840]
4. Kaech SM, Cui W. Transcriptional control of effector and memory CD8+ T cell differentiation. Nat Rev Immunol. 2012; 12(11):749–761. [PubMed: 23080391]
5. MacIver NJ, Michalek RD, Rathmell JC. Metabolic regulation of T lymphocytes. Annual review of immunology. 2013; 31:259–283.
6. van der Windt GJ, Pearce EL. Metabolic switching and fuel choice during T-cell differentiation and memory development. Immunological reviews. 2012; 249(1):27–42. [PubMed: 22889213]
7. Wang R, Green DR. Metabolic reprogramming and metabolic dependency in T cells. Immunol Rev. 2012; 249(1):14–26. [PubMed: 22889212]
8. Kim J, Woo AJ, Chu J, Snow JW, Fujiwara Y, Kim CG, et al. A Myc network accounts for similarities between embryonic stem and cancer cell transcription programs. Cell. 2010; 143(2): 313–324. [PubMed: 20946988]
9. Nie Z, Hu G, Wei G, Cui K, Yamane A, Resch W, et al. c-Myc is a universal amplifier of expressed genes in lymphocytes and embryonic stem cells. Cell. 2012; 151(1):68–79. [PubMed: 23021216]
10. Lin CY, Loven J, Rahl PB, Paranal RM, Burge CB, Bradner JE, et al. Transcriptional amplification in tumor cells with elevated c-Myc. Cell. 2012; 151(1):56–67. [PubMed: 23021215]
11. Rahl PB, Lin CY, Seila AC, Flynn RA, McCuine S, Burge CB, et al. c-Myc regulates transcriptional pause release. Cell. 2010; 141(3):432–445. [PubMed: 20434984]
12. Sinclair LV, Rolf J, Emslie E, Shi YB, Taylor PM, Cantrell DA. Control of amino-acid transport by antigen receptors coordinates the metabolic reprogramming essential for T cell differentiation. Nat Immunol. 2013; 14(5):500–508. [PubMed: 23525088]
13. Wang R, Dillon CP, Shi LZ, Milasta S, Carter R, Finkelstein D, et al. The transcription factor Myc controls metabolic reprogramming upon T lymphocyte activation. Immunity. 2011; 35(6):871–882. [PubMed: 22195744]
14. Kaech SM, Ahmed R. Memory CD8+ T cell differentiation: initial antigen encounter triggers a developmental program in naive cells. Nat Immunol. 2001; 2(5):415–422. [PubMed: 11323695]
15. Prlic M, Hernandez-Hoyos G, Bevan MJ. Duration of the initial TCR stimulus controls the magnitude but not functionality of the CD8+ T cell response. J Exp Med. 2006; 203(9):2135–2143. [PubMed: 16908626]
16. Blair DA, Turner DL, Bose TO, Pham QM, Bouchard KR, Williams KJ, et al. Duration of antigen availability influences the expansion and memory differentiation of T cells. J Immunol. 2011; 187(5):2310–2321. [PubMed: 21775679]
17. Porter BB, Harty JT. The onset of CD8+-T-cell contraction is influenced by the peak of Listeria monocytogenes infection and antigen display. Infect Immun. 2006; 74(3):1528–1536. [PubMed: 16495523]
18. Best JA, Blair DA, Knell J, Yang E, Mayya V, Doedens A, et al. Transcriptional insights into the CD8(+) T cell response to infection and memory T cell formation. Nat Immunol. 2013; 14(4):404–412. [PubMed: 23396170]
19. Williams MA, Tyznik AJ, Bevan MJ. Interleukin-2 signals during priming are required for secondary expansion of CD8+ memory T cells. Nature. 2006; 441(7095):890–893. [PubMed: 16778891]
20. Obar JJ, Molloy MJ, Jellison ER, Stoklasek TA, Zhang W, Usherwood EJ, et al. CD4+ T cell regulation of CD25 expression controls development of short-lived effector CD8+ T cells in primary and secondary responses. Proceedings of the National Academy of Sciences of the United States of America. 2010; 107(1):193–198. [PubMed: 19966302]
21. D'Souza WN, Lefrancois L. IL-2 is not required for the initiation of CD8 T cell cycling but sustains expansion. J Immunol. 2003; 171(11):5727–5735. [PubMed: 14634080]
22. Kalia V, Sarkar S, Subramaniam S, Haining WN, Smith KA, Ahmed R. Prolonged interleukin-2Ralpha expression on virus-specific CD8+ T cells favors terminal-effector differentiation in vivo. Immunity. 2010; 32(1):91–103. [PubMed: 20096608]

23. Pipkin ME, Sacks JA, Cruz-Guilloty F, Lichtenheld MG, Bevan MJ, Rao A. Interleukin-2 and inflammation induce distinct transcriptional programs that promote the differentiation of effector cytolytic T cells. Immunity. 2010; 32(1):79–90. [PubMed: 20096607]
24. Egawa T, Littman DR. Transcription factor AP4 modulates reversible and epigenetic silencing of the Cd4 gene. Proc Natl Acad Sci U S A. 2011; 108(36):14873–14878. [PubMed: 21873191]
25. Hu YF, Luscher B, Admon A, Mermod N, Tjian R. Transcription factor AP-4 contains multiple dimerization domains that regulate dimer specificity. Genes Dev. 1990; 4(10):1741–1752. [PubMed: 2123466]
26. Mermod N, Williams TJ, Tjian R. Enhancer binding factors AP-4 and AP-1 act in concert to activate SV40 late transcription in vitro. Nature. 1988; 332(6164):557–561. [PubMed: 2833704]
27. Maekawa Y, Minato Y, Ishifune C, Kurihara T, Kitamura A, Kojima H, et al. Notch2 integrates signaling by the transcription factors RBP-J and CREB1 to promote T cell cytotoxicity. Nat Immunol. 2008; 9(10):1140–1147. [PubMed: 18724371]
28. Pircher H, Burki K, Lang R, Hengartner H, Zinkernagel RM. Tolerance induction in double specific T-cell receptor transgenic mice varies with antigen. Nature. 1989; 342(6249):559–561. [PubMed: 2573841]
29. Yoon H, Kim TS, Braciale TJ. The cell cycle time of CD8+ T cells responding in vivo is controlled by the type of antigenic stimulus. PloS one. 2010; 5(11):e15423. [PubMed: 21079741]
30. Petersen LR, Fischer M. Unpredictable and difficult to control--the adolescence of West Nile virus. N Engl J Med. 2012; 367(14):1281–1284. [PubMed: 23013055]
31. Suthar MS, Diamond MS, Gale M Jr. West Nile virus infection and immunity. Nat Rev Microbiol. 2013; 11(2):115–128. [PubMed: 23321534]
32. Shrestha B, Diamond MS. Role of CD8+ T cells in control of West Nile virus infection. J Virol. 2004; 78(15):8312–8321. [PubMed: 15254203]
33. Wang R, Green DR. Metabolic checkpoints in activated T cells. Nat Immunol. 2012; 13(10):907–915. [PubMed: 22990888]
34. Jung P, Menssen A, Mayr D, Hermeking H. AP4 encodes a c-MYC-inducible repressor of p21. Proceedings of the National Academy of Sciences of the United States of America. 2008; 105(39): 15046–15051. [PubMed: 18818310]
35. Huang CYB AL, Walker LM, Bassing CH, Sleckman BP. Dynamic regulation of c-Myc proto-oncogene expression during lymphocyte development revealed by a GFP-c-Myc knock-in mouse. Eur J Immunol. 2008; 38(2):342–349. [PubMed: 18196519]
36. van der Windt GJ, Everts B, Chang CH, Curtis JD, Freitas TC, Amiel E, et al. Mitochondrial respiratory capacity is a critical regulator of CD8+ T cell memory development. Immunity. 2012; 36(1):68–78. [PubMed: 22206904]
37. Loven J, Orlando DA, Sigova AA, Lin CY, Rahl PB, Burge CB, et al. Revisiting global gene expression analysis. Cell. 2012; 151(3):476–482. [PubMed: 23101621]
38. Chang DW, Claassen GF, Hann SR, Cole MD. The c-Myc transactivation domain is a direct modulator of apoptotic versus proliferative signals. Molecular and cellular biology. 2000; 20(12): 4309–4319. [PubMed: 10825194]
39. Yeh E, Cunningham M, Arnold H, Chasse D, Monteith T, Ivaldi G, et al. A signalling pathway controlling c-Myc degradation that impacts oncogenic transformation of human cells. Nature cell biology. 2004; 6(4):308–318. [PubMed: 15048125]
40. de Alboran IM, O'Hagan RC, Gartner F, Malynn B, Davidson L, Rickert R, et al. Analysis of C-MYC function in normal cells via conditional gene-targeted mutation. Immunity. 2001; 14(1):45–55. [PubMed: 11163229]
41. Ventura A, Kirsch DG, McLaughlin ME, Tuveson DA, Grimm J, Lintault L, et al. Restoration of p53 function leads to tumour regression in vivo. Nature. 2007; 445(7128):661–665. [PubMed: 17251932]
42. Zehn D, Lee SY, Bevan MJ. Complete but curtailed T-cell response to very low-affinity antigen. Nature. 2009; 458(7235):211–214. [PubMed: 19182777]
43. Hogquist KA, Jameson SC, Heath WR, Howard JL, Bevan MJ, Carbone FR. T cell receptor antagonist peptides induce positive selection. Cell. 1994; 76(1):17–27. [PubMed: 8287475]

44. Mombaerts P, Clarke AR, Rudnicki MA, Iacomini J, Itohara S, Lafaille JJ, et al. Mutations in T-cell antigen receptor genes alpha and beta block thymocyte development at different stages. Nature. 1992; 360(6401):225–231. [PubMed: 1359428]

45. Willerford DM, Chen J, Ferry JA, Davidson L, Ma A, Alt FW. Interleukin-2 receptor alpha chain regulates the size and content of the peripheral lymphoid compartment. Immunity. 1995; 3(4):521–530. [PubMed: 7584142]

46. Morita S, Kojima T, Kitamura T. Plat-E: an efficient and stable system for transient packaging of retroviruses. Gene Ther. 2000; 7(12):1063–1066. [PubMed: 10871756]

47. Bolstad BM, Irizarry RA, Astrand M, Speed TP. A comparison of normalization methods for high density oligonucleotide array data based on variance and bias. Bioinformatics. 2003; 19(2):185–193. [PubMed: 12538238]

48. Ciofani M, Madar A, Galan C, Sellars M, Mace K, Pauli F, et al. A validated regulatory network for Th17 cell specification. Cell. 2012; 151(2):289–303. [PubMed: 23021777]

49. Langmead B, Salzberg SL. Fast gapped-read alignment with Bowtie 2. Nat Methods. 2012; 9(4): 357–359. [PubMed: 22388286]

50. Heinz S, Benner C, Spann N, Bertolino E, Lin YC, Laslo P, et al. Simple combinations of lineage-determining transcription factors prime cis-regulatory elements required for macrophage and B cell identities. Molecular cell. 2010; 38(4):576–589. [PubMed: 20513432]

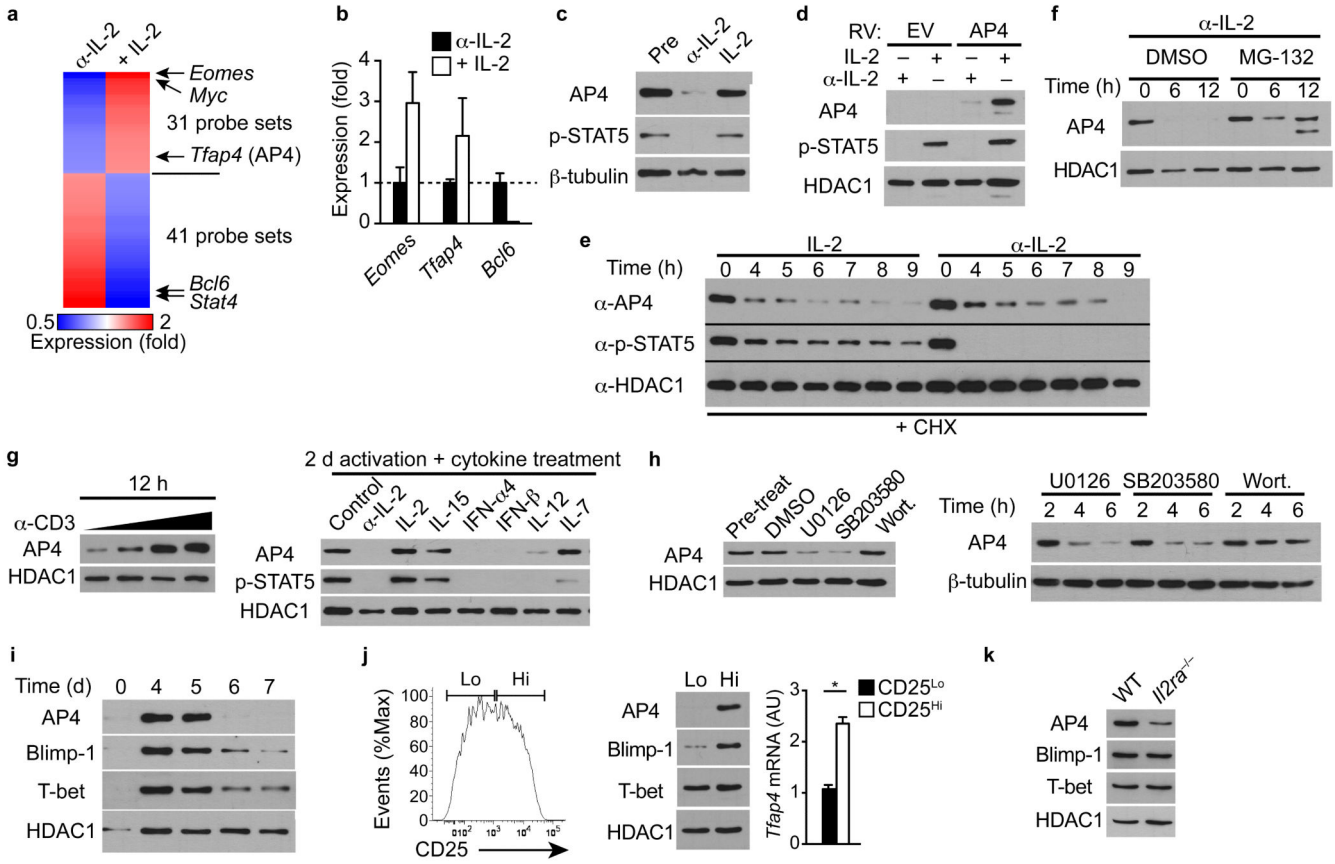

Figure 1.

AP4 is post-transcriptionally regulated in CD8$^+$ T cells. (**a**) Mean microarray signal intensity for TFs differentially expressed (>1.8-fold) in activated CD8$^+$ T cells treated with IL-2 (100 U/ml) or anti-IL-2 antibody (2 μg/ml) for 12 h. (*n* =3). (**b**) qRT-PCR analysis showing expression levels of indicated genes in CD8$^+$ T cells treated as in (**a**). Error bars, s.d. (*n* = 2). (**c**) Immunoblot showing AP4 expression in CD8$^+$ T cells treated as in (**a**). Phosphorylated STAT5 and β-tubulin serve as controls. (*n* = 4). (**d**) Immunoblot showing AP4 expression in IL-2-treated or IL-2-deprived *Tfap4*$^{-/-}$ CD8$^+$ T cells transduced with an empty (EV) or AP4-expressing RV. (*n* = 2). (**e**) Immunoblot analysis of AP4 in IL-2-treated or IL-2-deprived CD8$^+$ T cells in the presence of cycloheximide (CHX, 10 μM) for indicated time. (*n* = 2). (**f**) Immunoblot analysis of AP4 in IL-2-deprived CD8$^+$ T cells in the presence of MG-132 (10 μM) for indicated time. (*n* = 2). (**g**) Immunoblot analysis of AP4 in CD8$^+$ T cells stimulated with different concentrations of anti-CD3 antibody for 12 h (left, *n* = 2) or with indicated cytokines for 12 h after 2 day stimulation with anti-CD3 antibody (right, *n* = 2). (**h**) Immunoblot analysis of AP4 in CD8$^+$ T cells stimulated with anti-CD3 and anti-CD28 antibodies for 48 h followed by treatments with indicated chemicals for 6 h (left, *n* = 2) and in those treated with chemicals after IL-2 stimulation for 24 h following anti-CD3 and anti-CD28 antibody stimulation (right, *n* = 2). Wort: Wortmannin. (**i**) Immunoblot analysis of AP4, Blimp-1 and T-bet in adoptively transferred P14 T cells at indicated time points after LCMV-Arm infection. (**j**) Histogram showing CD25 expression in CD8$^+$ CD44$^+$ CD62L$^-$ T cells in B6 mice on day 4.5 after LCMV-Arm infection (left), immunoblots

showing AP4, Blimp-1 and T-bet expression (middle), and qRT-PCR analysis showing *Tfap4* expression (right) in $CD25^{Lo}$ and $CD25^{Hi}$ cells. (n =2). Error bars, s.d. (**k**) Immunoblots showing AP4 expression in $Il2ra^{-/-}$ P14 T cells on day 4 post LCMV-Arm infection. (n = 2). * $P < 0.05$ by unpaired t-test.

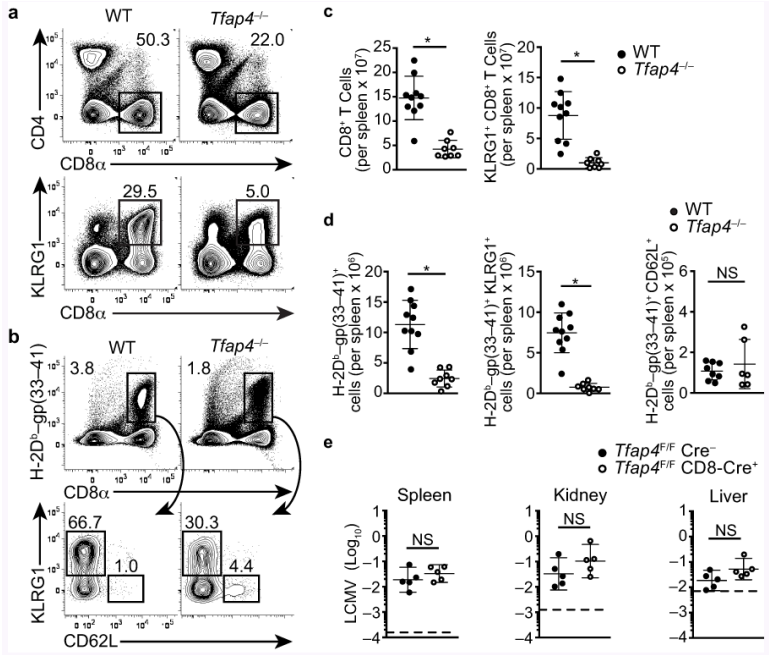

Figure 2. AP4 is required for expansion of Ag-specific CD8$^+$ T cells following LCMV-Arm infection. (**a,b**) Flow cytometry of splenocytes from *Tfap4*$^{-/-}$ and WT mice 8 days after LCMV infection showing CD4, CD8, KLRG1 and CD62L expression and binding of an H-2D^b–gp(33–41) tetramer. Percentages of CD8$^+$ T cells, CD8$^+$ KLRG1$^+$ effector cells, and gp(33–41)-specific CD8$^+$ T cells of the total splenocytes (top panels) and percentages of CD62L$^+$ and KLRG1$^+$ cells in gp(33–41)-specific CD8$^+$ T cells (bottom panels) are shown with gates indicated as rectangles. Statistical analysis of data from ten WT and eight *Tfap4*$^{-/-}$ mice from three experiments is shown in (**c**) and (**d**). (**e**) qRT-PCR analysis of the LCMV GP transcript in spleen, kidney, and liver of *Tfap4*$^{F/F}$ CD8-Cre$^+$ and control *Tfap4*$^{F/F}$ Cre$^-$ mice 6 days after LCMV-Arm infection. Transcript levels were normalized against *Hprt1* levels. Data from five mice in two experiments were combined. Dotted lines indicate the limit of detection. Error bars, s.d. * $P < 0.0001$ by unpaired *t*-test. NS: not significant.

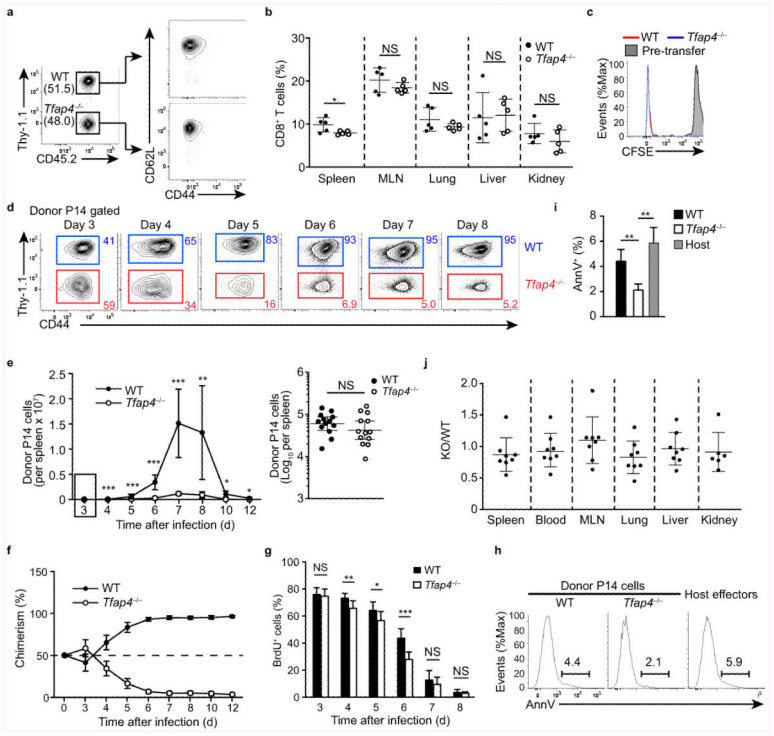

Figure 3.

AP4 is required for sustained CD8 clonal expansion but not for initial proliferation. (**a**) Flow cytometry of *Tfap4*$^{-/-}$ (Thy-1.1^{-} CD45.2) and control WT (Thy-1.1^{+} CD45.2) P14 T cells 16 h after co-transfer at a 1:1 ratio into congenic host mice showing expression of Thy-1.1, CD45.2, CD62L and CD44. (*n* = 3). (**b**) Frequencies of CD8^{+} T cells in the spleen, mesenteric lymph nodes (MLN), lung, liver, and kidney of *Tfap4*$^{-/-}$ and control B6 mice under steady-state conditions. (*n* = 5). **(c)** Flow cytometry of CFSE-labeled *Tfap4*$^{-/-}$ and WT P14 T cells in host mice three days after LCMV-Arm infection. (*n* = 2). (**d**) Flow cytometry showing the frequencies of *Tfap4*$^{-/-}$ and WT P14 donor cells at different time points after LCMV-Arm infection in host mice with a starting ratio of 1:1. (**e-g**) Statistical analysis of numbers of *Tfap4*$^{-/-}$ and WT P14 cells in the spleen normalized to 10,000 transferred cells (**e**), ratios between *Tfap4*$^{-/-}$ and WT P14 T cells (**f**), and percentages of BrdU^{+} cells following two hour pulse labeling (**g**). (*n* = 9-13 for day 3, 8-18 for day 4, 8-13 for day 5, 9-19 for day 6, 4-8 for day 7, 4-9 day 8, 3 for day 10, 5 for day 12). (**h,i**) Flow cytometry of transferred *Tfap4*$^{-/-}$ and WT P14 cells and host CD8^{+}CD44^{+} cells in the spleen six days after LCMV-Arm infection showing AnnexinV (AnnV) binding. Representative plots (**h**) and statistical analysis from five mice (**i**) are shown. (**j**) Relative frequencies of *Tfap4*$^{-/-}$ and WT P14 donor cells in different organs and blood in host mice seven days after LCMV-Arm infection with a starting ratio of 6:1. (*n* = 8). Error bars, s.d. * $P < 0.05$, ** $P < 0.01$, *** $P < 0.001$ by unpaired *t*-test. NS: not significant by unpaired *t*-test (**b**, **e**, **g**) and by one-way ANOVA (**j**).

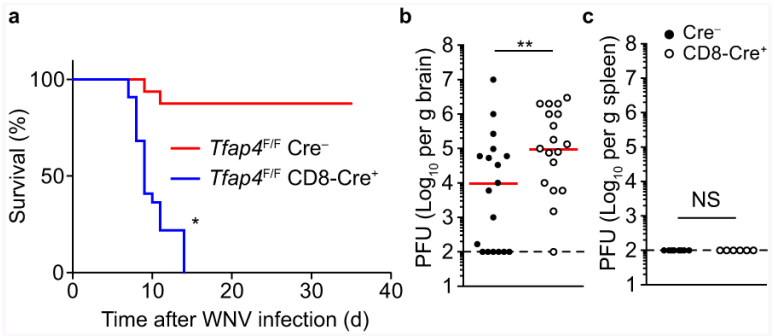

Figure 4.

AP4 is essential for host protection against WNV infection in a CD8$^+$ T cell-intrinsic manner. (**a**) Survival of *Tfap4*$^{F/F}$ CD8-Cre$^+$ and control *Tfap4*$^{F/F}$ Cre$^-$ mice following WNV infection. Data from three independent experiments were pooled (n = 22 for CD8-Cre$^+$, n = 16 for Cre$^-$). * $P < 0.001$ by the log-rank test. (**b,c**) Viral titers in the brain (**b**) and spleen (**c**) from *Tfap4*$^{F/F}$ CD8-Cre$^+$ and control *Tfap4*$^{F/F}$ Cre$^-$ mice on day 9 post-WNV infection. Data were pooled from four (**b**, n = 18) or two (**c**, n = 7) independent experiments. Red bars in (**b**) indicate median values of PFU/gram tissue. ** $P < 0.05$, NS: not significant by Mann Whitney U-test.

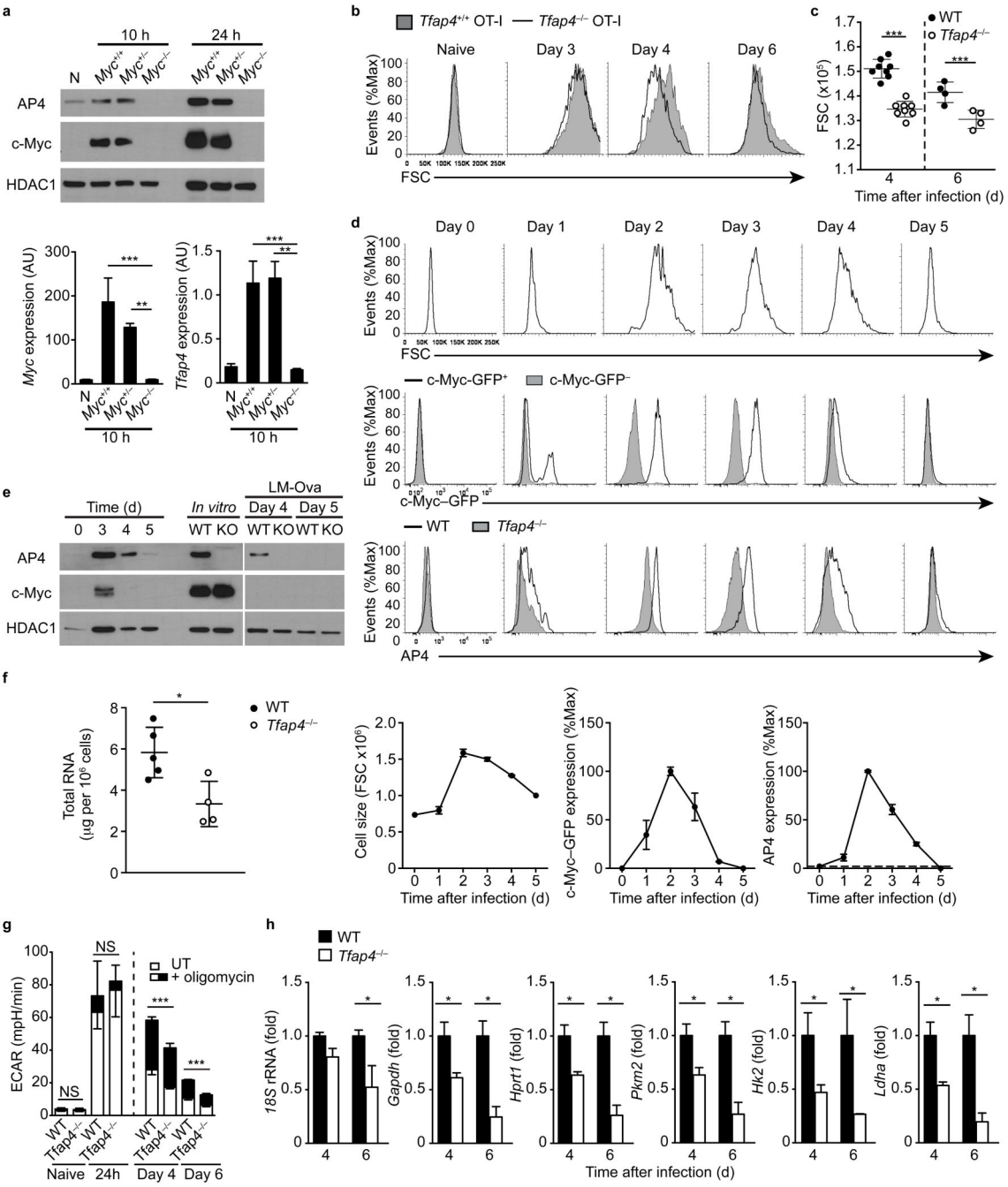

Figure 5.

AP4 is induced by c-Myc and sustains glycolysis. **(a)** Immunoblot and qRT-PCR analysis showing AP4 and c-Myc expression in CD8$^+$ T cells following a 4OHT treatment and stimulation for 10 or 24 h *in vitro*. *Myc*$^{+/+}$: *Myc*$^{F/+}$ Cre$^-$, Myc$^{+/-}$: *Myc*$^{F/+}$ CreER^{T2}(+), Myc$^{-/-}$: *Myc*$^{F/F}$ CreER^{T2}(+), N: 4OHT-treated WT naive CD8$^+$ T cells. (n = 3). (**b,c**) Flow cytometry of OT-I T cells showing FSC after Lm-Ova infection (**b**) with statistical analysis (**c**). (n = 8 for day 4, 4 for day 6). **(d)** Flow cytometry analysis of c-Myc-GFP and AP4 expression in OT-I T cells following Lm-Ova infection. c-Myc-GFP levels were determined

by subtracting the autofluorescence from the GFP fluorescence of *Myc*$^{c\text{-}Myc\text{-}GFP/+}$ OT-I T cells. FSC of WT OT-I T cells is shown as a reference. (n = 1 for day 0, 3 for days 1 to 3, 2 for days 4 and 5). (**e**) Immunoblot showing c-Myc and AP4 expression in OT-I T cells after Lm-Ova infection. Lysates from *Tfap4*$^{-/-}$ CD8^{+} T cells were used to show antibody specificity. (n = 3). (**f**) Total RNA content in OT-I T cells four days after Lm-Ova infection. (n = 5 for WT, 4 for *Tfap4*$^{-/-}$). (**g**) ECAR measurement of CD8^{+} T cells without stimulation (naive), after 24 h stimulation *in vitro*, or on days 4 and 6 after Lm-Ova infection. Baseline values (UT) and changes following treatment with oligomycin are shown. (n = 6 for naive, 10 for 24 h, 3 for days 4 and 6). (**h**) qRT-PCR analysis of expression of glycolytic genes in OT-I T cells. Expression levels were normalized against the ERCC-00108 spiked-in control RNA and shown as relative values to WT OT-I T cells (n = 2 for day 4 WT and day 6 *Tfap4*$^{-/-}$, 3 for day 4 *Tfap4*$^{-/-}$ and day 6 WT). Error bars, s.d. * P < 0.05, ** P < 0.01, *** P < 0.001, NS: not significant by one-way ANOVA (**a**), paired (**c**) or unpaired t-test (**f**-**h**).

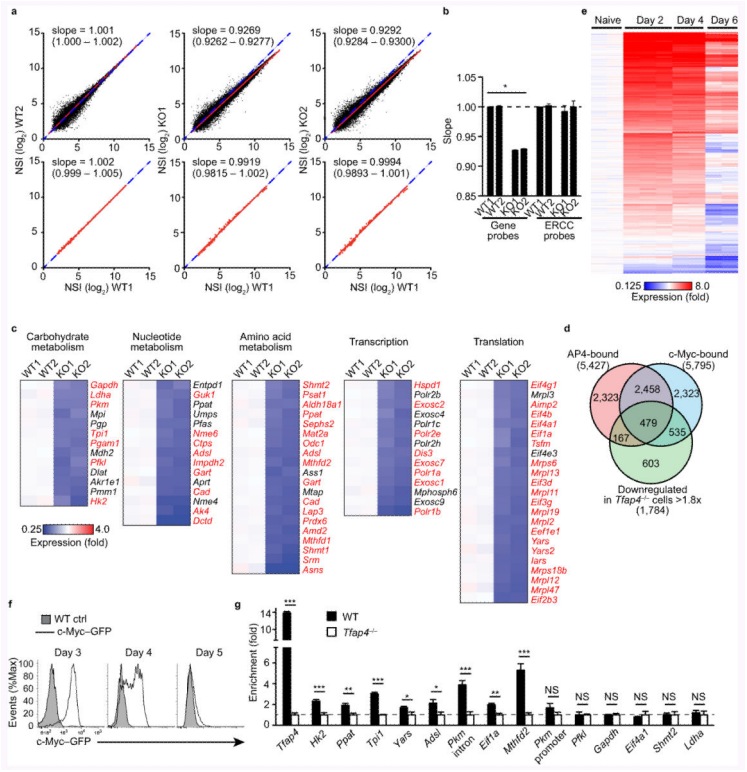

Figure 6.

AP4 is essential for sustained expression of c-Myc target genes. (**a, b**) Scatter plots showing normalized signal intensity (NSI) of endogenous transcripts in *Tfap4*$^{-/-}$ (KO) and WT OT-I T cells on day 4 after Lm-Ova infection (upper panels) and ERCC control RNA (bottom panels). Values of slopes obtained by linear regression (95% CI in parentheses) are shown. The slope of the blue dotted line in each plot is 1. Error bars, 95% CI in (**b**). (**c**) Heat maps showing expression of genes in over-represented pathways identified by NIH DAVID ver. 6.7 (n = 2). Genes shown in red are bound by both c-Myc and AP4. (**d**) Venn diagram showing overlap between AP4-bound genes, c-Myc-bound genes and differentially expressed genes. (**e**) Expression kinetics of the 479 genes defined in (**d**) in WT OT-I T cells after Lm-Ova infection. Expression levels were normalized to values in naive CD8^{+} T cells. (n = 2 for naive, days 4 and 6, 3 for day 2). (**f**) Flow cytometry of *Myc*$^{\text{c-Myc-GFP}}$ P14 T cells showing c-Myc-GFP expression after LCMV-Arm infection. (n = 4). (**g**) ChIP-qPCR analysis of AP4 binding to AP4-c-Myc co-targeted genes in P14 T cells on day 5 after LCMV-Arm infection. Data normalized to signals from *Tfap4*$^{-/-}$ cells. Error bars, s.d. *P < 0.05, **P < 0.01, ***P < 0.001, NS: not significant by unpaired t-test.

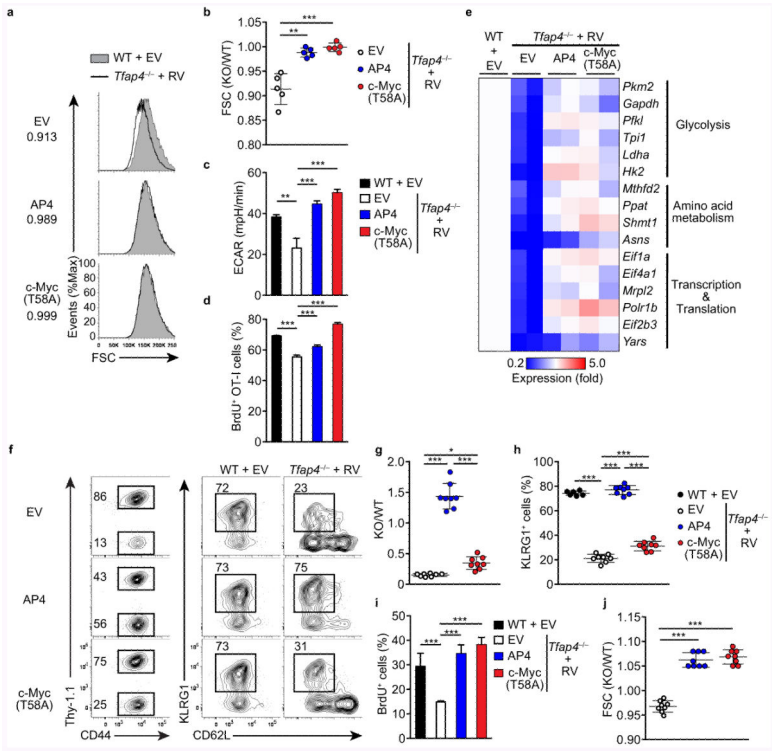

Figure 7.

Sustained c-Myc expression rescues defects of *Tfap4*$^{-/-}$ CD8 T cells. (**a**) Flow cytometry of *Tfap4*$^{-/-}$ OT-I T cells transduced with empty (EV), AP4- or c-Myc(T58A)-expressing RV showing FSC. Co-cultured EV-transduced WT OT-I T cells were used as control. Statistical analysis of FSC ratios between RV-transduced *Tfap4*$^{-/-}$ and EV-transduced WT OT-I T cells are shown in (**b**). (n = 5). **(c,d)** ECAR (**c**) and BrdU incorporation rates (**d**) of RV-transduced *Tfap4*$^{-/-}$ and EV-transduced control WT OT-I T cells. (n = 3). (**e**) qRT-PCR analysis of expression of AP4-c-Myc co-target genes in RV-transduced *Tfap4*$^{-/-}$ and EV-transduced WT OT-I T cells. Expression of each gene was normalized against the control ERCC-108 spiked-in RNA and shown as a heat map. (n = 2). (**f**) Flow cytometry showing frequencies of and expression of Thy-1.1, CD44, KLRG1 and CD62L in adoptively co-transferred RV-transduced *Tfap4*$^{-/-}$ (Thy1.1^{-}) and EV-transduced WT (Thy-1.1^{+}) OT-I T cells on day 6 after Lm-Ova infection. (n = 8). (**g-j**) Statistical analyses of relative frequencies of RV-transduced *Tfap4*$^{-/-}$ to EV-transduced WT OT-I T cells (KO/WT, **g**) and percentages of KLRG1^{+} cells (**h**), BrdU incorporation rates (**i**), and FSC ratios between RV-transduced *Tfap4*$^{-/-}$ and co-transferred EV-transduced WT OT-I T cells (**j**). (n = 8 for **g, h, j**, 4 for **i**). Error bars, s.d. * $P < 0.05$, * $P < 0.01$, *** $P < 0.001$ by one-way ANOVA.